Beyond Scalar Timing Theory: Integrating Neural Oscillators with Computational Accessibility in Memory[‡]

Zhuanghua Shi[1,*], Bon-Mi Gu[2], Stefan Glasauer[3] and Warren H. Meck[†,4]

[1] Department of Experimental Psychology, Ludwig Maximilian University of Munich, Munich, Germany

[2] Department of Neurology and Neurological Sciences, Stanford University, Stanford, CA 94305, USA

[3] Chair of Computational Neuroscience, Brandenburg University of Technology Cottbus, Germany

[4] Department of Psychology and Neuroscience, Duke University, Durham, NC, USA

[‡] We dedicate this paper to Warren H. Meck, who raised the following important issue back in 2017: there is a gap between two major classes of timing models — the ramping-based accounts (such as scalar timing theory, drift–diffusion models) and the oscillatory models (e.g., striatal beat-frequency model). Through our conversation, we all felt most existing timing models are specific for prospective timing, lacking a generative prediction for retrospective timing. In particular, those models lack computational accessibility, which is needed for solving the retrospective mapping problem. The model we propose here, which was first developed before Warren left us, attempts to address this issue.

[†] Deceased.

[*] To whom correspondence should be addressed. E-mail: strongway@psy.lmu.de

Beyond Scalar Timing Theory

30 **Abstract**

31 One of the major challenges for computational models of timing and time perception is to identify a neurobiological
32 plausible implementation that predicts various behavioral properties, including the scalar property and retrospective
33 timing. The available timing models primarily focus on the scalar property and prospective timing, while virtually
34 ignoring the computational accessibility. Here, we first selectively review timing models based on ramping activity,
35 oscillatory pattern, and time cells, and discuss potential challenges for the existing models. We then propose a
36 multifrequency oscillatory model that offers computational accessibility, which could account for a much broader range
37 of timing features, including both retrospective and prospective timing.

38 **Keywords**

39 Interval timing, retrospective timing, prospective timing, computational accessibility, neural oscillators, memory

40

1. Introduction

41

42

43 One key feature of interval timing, the scalar property, is that the estimation error, measured by the

44 standard deviation, scales linearly with the magnitude of the estimated interval, approximately

45 following Weber's law. The scalar property was first incorporated into the scalar timing theory

46 (STT) — an information-processing model of the internal clock (Church, 2003; Church et al., 1994;

47 Gibbon, 1977; Gibbon et al., 1984). The STT proposes that interval timing comes from the

48 interaction of three processing stages: a central clock, memory, and a decision process. At the clock

49 level, a pacemaker generates raw time representation "ticks" through a Poisson process, mimicking

50 neuronal spike trains. Those ticks pass through a switch to an accumulator. At the onset of a timed

51 stimulus, the switch closes, allowing the accumulator to count the raw ticks until the switch opens.

52 It then transfers the accumulated ticks to working memory, representing the timed interval. At the

53 final stage, the timed interval is compared with a long-term memory representation of biologically

54 important intervals. The original STT successfully predicts many results in animal timing (Gibbon,

55 1977; Gibbon et al., 1984; Meck, 1983), as well as behavioral timing from humans (Allman et al.,

56 2014, 2016; Buhusi & Meck, 2005).

57 The key ingredient of the STT is the scalar property. Using a linear accumulator, Gibbon

58 and colleagues (1992) have noticed that the first passage time T at a constant threshold only

59 produces a gamma distribution if the variances mainly come from the Poisson clock and the

60 decision stage. The ratio of the standard deviation over the mean interval from the gamma

61 distribution, however, does not generate constant scalar property. To amend this, Gibbon and

62 colleagues argued that the scalar property is likely caused by the variability from the memory

63 translation of the accumulated 'ticks' (Gibbon, 1977; Gibbon et al., 1984). Recently Beck and

64 colleagues (2012) also reached a similar conclusion, suggesting that a global nuisance correlation

65 in memory representation is a potential cause of the scalar property.

66 Although the information-processing STT can successfully account for a large proportion

67 of the behavioral data, the model has been criticized for its lack of neurophysiologically plausible

68 implementation (e.g., Allman et al., 2014; Buhusi & Meck, 2005). Over the past few decades,

69 researchers have developed multiple timing theories, varying from the original information-

70 processing STT (Church, 2003; Church et al., 1994; Gibbon, 1977; Gibbon et al., 1984), to the

71 behavioral theory of timing (BeT) (Killeen & Fetterman, 1988) and the Spectral Timing Model

72 (Grossberg & Merrill, 1992, 1996; Grossberg & Schmajuk, 1989), to neurobiological plausible

73 models, such as the striatal beat-frequency (SBF) (Matell & Meck, 2004; Oprisan & Buhusi, 2011),

74 opponent Poisson drift–diffusion process (opDDM) (Balcı & Simen, 2014; Simen et al., 2011),

75   state-dependent neural networks (Buonomano, 2000; Goel & Buonomano, 2014), and cerebellar,

76   hippocampal, and striatal time cells (Eichenbaum, 2014; Lusk et al., 2016; MacDonald et al., 2011,

77   2014). Based on the representation of time, we can roughly categorize interval timing theories into

78   the ramping accumulation, state-dependent, delay-line, neural oscillators, memory-based models

79   (Addyman et al., 2016; Hardy & Buonomano, 2016; Hass & Durstewitz, 2016), and time cells

80   (Eichenbaum, 2014; MacDonald et al., 2011; Rolls & Mills, 2019). Here, we selectively review

81   three major classes of neurobiological plausible timing accounts and empirical findings of interval

82   timing behaviors that challenge those accounts. We then further propose an integrated model that

83   incorporates multifaceted timing features for both prospective and retrospective timing.

84

85   ## 2. Ramping Accumulation, Oscillatory Models and Time Cells

86

87   One implicit assumption of classical internal clock models is that the accumulator linearly

88   accumulates 'ticks' (Gibbon, 1977; Gibbon et al., 1984). Given that a long interval requires more

89   resources than a short interval, the accumulator needs unbound capacity for extremely long

90   intervals, which is unlikely to be implemented in biological organisms. Instead of using simple

91   linear accumulation, recent neural integration models, such as the opDDM (Balcı & Simen, 2014;

92   Simen et al., 2011, 2016), adopt stochastic ramping activity as the temporal integrator, which starts

93   at the beginning of the interval and consistently increases till the end of the interval. The stochastic

94   ramping process is the central key element of drift–diffusion models (DDMs), which have been

95   widely applied to reaction-time paradigms (Chen et al., 2021; e.g., Ratcliff et al., 2003) on studying

96   temporal cognition (Matthews & Meck, 2016). Ramping is also a common pattern of neuronal

97   activity in the frontal cortex (Parker et al., 2014), the lateral intraparietal (LIP) area (Jazayeri &

98   Shadlen, 2015), and the posterior insular cortex (Wittmann et al., 2010) during temporal decision-

99   making (for a review, see Narayanan, 2016). More recently, ramping temporal cells have been

100 shown in the lateral entorhinal cortex (Tsao et al., 2018). The opDDM assumes the decision variable

101 of a timing process is represented by the difference of spike counts from two Poisson processes.

102 For a single timing task, the opDDM reduces to one Poisson process, which is similar to the STT

103 model. One critical feature of the opDDM that differs from the STT is that the opDDM assumes

104 the ramping activity reaches a fixed decision barrier at a specific temporal criterion (e.g., when

105 subjects get rewards with their response, such as pressing a lever). By using a fixed decision barrier

106 across different durations, an assumption originated from BeT (Killeen & Fetterman, 1988), the

107 opDDM nicely avoids the unbound problem. In addition, it produces time scale invariance as long

108 as the decision barrier is constant. However, this fixed decision barrier comes at a cost. The drift

109   rate (internal Poisson clock speed) must be varied across different durations. The longer the duration

110   is, the lower the drift rate (clock speed) must be. Although the models can capture various features

111   from interval timing, such as one-trial learning (Simen et al., 2011) and learning of cyclically

112   varying time intervals (Luzardo et al., 2017), under the assumption of varied drift rates across

113   different durations, the explanatory power of the opDDM is limited to prospective timing for

114   individual to-be-timed intervals. The model falls short for timing retrospective intervals with

115   unknown onsets.

116   Instead of adopting ramping representation, oscillator timing models, such as the oscillatory

117   striatal beat-frequency model (SBF, Matell & Meck, 2000, 2004; Oprisan & Buhusi, 2011),

118   consider the oscillatory firing patterns of cortical neurons as interval encoders. The SBF model

119   assumes cortical oscillatory neurons with rates ranging between 5 and 15 Hz synchronize to the

120   onset of relevant stimuli driven by dopamine release from the ventral tegmental area (VTA) (Matell

121   & Meck, 2000, 2004). Those cortical oscillatory activities, which change over time, are transmitted

122   to medium spiny neurons (MSNs) in the basal ganglia. Through temporal learning, the synaptic

123   weights between MSNs and cortical neurons with different endogenous oscillatory periods are

124   formed for coincidence detection of the duration encoded by the MSNs. A time interval is detected

125   by the similarity between the oscillatory pattern and the pattern of the comparison interval stored

126   in the memory. Given that each spiny neuron receives tens of thousands of inputs from cortical

127   neurons, this level of convergence permits coding suprasecond intervals with integrating a few

128   primitives represented by different subsecond oscillation frequencies in the cortex. The SBF model

129   assumes variations in global oscillation frequencies (similar to the between-trial variations in clock

130   speeds used in STT) and variations in the start and stop response thresholds, which lead to scalar

131   behavior in the cortical coherence function (Matell & Meck, 2004). Several recent oscillatory

132   models extend the original SBF in various aspects. For instance, replacing oscillators with

133   biophysically realistic and noisy Morris–Lecar neurons (SBF-ML) can explain the pharmacological

134   clock and memory patterns observed in the literature (Buhusi & Oprisan, 2013; Oprisan & Buhusi,

135   2011). Using coupled excitatory–inhibitory oscillation (EIO), Gu and colleagues (2015) unified a

136   shared oscillatory process of interval timing and working memory; both are inextricably

137   intermingled. The extension permits the model to store multiple intervals in the working memory

138   with an overlapping ensemble of EIO oscillators, offering a possibility of how multiple temporal

139   intervals are encoded simultaneously (De Corte & Matell, 2016a; Merchant et al., 2008). Both SBF-

140   ML and EIO models share the same coincidence detection mechanism that is proposed in the

141   original SBF for identifying a target interval (Matell & Meck, 2000): a set of oscillatory neurons

142   synchronize at the onset of a to-be-timed interval, and the pattern at the offset of the interval is

143   stored in the memory system. Like those ramping accumulation models, oscillatory models are

144   primarily suitable for prospective timing.

145   It is worth noting that one early multiple-oscillator model uses a slightly different approach

146   (Church & Broadbent, 1990). In the multiple-oscillator model, oscillators vary from very low to

147   high frequencies, equally sampled from a log-space (e.g., 0.1, 0.2, 0.4 Hz…), analogous to multiple

148   slow to fast pacemakers. It is assumed that human and other animals could not retrieve the precise

149   phase of an oscillator, rather merely the half-phase (i.e., binary states). A set of phases, however,

150   can represent time. The reinforced interval is detected by similarity measures between the

151   represented interval and the retrieved reference memory (Church & Broadbent, 1990). The proposal

152   of the multiple-oscillator model shares some similarity to the spectral timing model (Grossberg &

153   Merrill, 1996; Grossberg & Schmajuk, 1989) to cover a wide range of time intervals. Instead of

154   using multifrequency oscillators, the spectral timing model assumes a population of neurons that

155   reacts to a stimulus at different times. Through reinforcement learning, the teaching signal (i.e., the

156   unconditioned stimulus) can change the weights of neurons, such that the population sum of the

157   activities can time the to-be-learned interval properly. However, the multiple-oscillator model is

158   special in terms of interval encoding. Unlike arbitrary patterns used in other oscillatory models, the

159   oscillatory pattern is much like our binary coding system, maintaining temporal distances among

160   represented intervals computationally accessible. Using oscillators with relatively low frequencies,

161   the multiple-oscillator model can encode long range intervals, such as minutes, hours, and days. In

162   fact, recent studies (Rolls & Mills, 2019; Tsao et al., 2018) suggest that the neurons that encode

163   time in the lateral entorhinal cortex have long-firing-rate timescales and using integrate-and-fire

164   attractor neural networks; the oscillatory excitation and inhibition can be over minutes. The

165   excitation and inhibition of two opponent neurons in the attractor network can also mimic the half-

166   phase changes in oscillatory networks. Studies have also shown animals can target specific hours

167   in a day (for a review, see Gallistel & King, 2009), suggesting that animals at least use some sort

168   of low-oscillatory timekeepers, including circadian rhythm, for tracking long intervals.

169   Recent studies on striatum, cerebellum, entorhinal cortex, and hippocampal neurons have

170   revealed the existence of time cells that fire at successive moments in temporally structured

171   experiences (Eichenbaum, 2014; MacDonald et al., 2011). The evidence comes from the firing

172   patterns of ensembles of hippocampal Cornu Ammonis area 1 (CA1) neurons in rats gradually

173   changing over the entire testing session, and even when the position of the animal was relatively

174   constant (Eichenbaum, 2017; MacDonald et al., 2011). More interestingly, time cells in CA1 exhibit

175   scalar properties. Time cells that fire later in a sequence also fire for a longer period. The

176   hippocampus is largely involved in episodic memory and encodes information based upon the

177   temporal organization of events, which makes the hippocampus an ideal brain structure for discrete
178   time events and retrospective timing (Issa et al., 2020; Lusk et al., 2016; MacDonald et al., 2014).
179   One distinguishing feature of the time cells is that timing is encoded by a sequential activation of
180   firing chains that are likely generated by an internally driven sequence within the hippocampal
181   circuitry (Buzsáki & Llinás, 2017). The ordinal sequences in the firing chains can represent the
182   past, present, and future (Frankland & Bontempi, 2005; Buzsáki & Llinás, 2017), permitting
183   temporal-order comparison and potential arithmetic comparison among different intervals. Friston
184   and Buzsáki (2016) further suggested that the internally driven sequence could purely encode time
185   without reference to any particular events. Such functional segregation of 'when' from 'what' and
186   'where' would be more efficient to encode when an event occurs than every combination of when,
187   what and where together. The content of the sequence depends on how events are 'bound' to
188   content-free temporal sequences through context-sensitive association (Friston & Buzsáki, 2016).
189   In this perspective, the sequence of firing chains of time cells could be regarded as timestamps
190   stamping events with their own ordinal structure. Recently, Rolls and Mills (2019) further suggested
191   that connections between events and time representation in hippocampal neurons are converted
192   from ramping time cells in the lateral entorhinal cortex, with the latter serving as intrinsic clocks.

193   Despite different approaches, those timing models successfully account for multiple
194   empirical findings from neuronal to behavioral levels. The ramping process can well predict the
195   behavioral response distributions (e.g., the inverse Gaussian distribution by the opDDM; Balcı &
196   Simen, 2014; Simen et al., 2011, 2016), and is observed in the posterior insular cortex during
197   temporal decision-making (Wittmann et al., 2010) and in the lateral entorhinal cortex (Tsao et al.,
198   2018). The opDDM can further correctly predict a level of skew that is approximately three times
199   the coefficient of variation (Simen et al., 2016). The neural oscillator models, on the other hand,
200   are grounded in neuronal networks of timing system in the brain, and consistent with the anatomical,
201   behavioral, and pharmacological evidence (Allman & Meck, 2012; Coull et al., 2010; Merchant et
202   al., 2013). The EIO model (Gu et al., 2015), for example, is constructed such that its mechanisms
203   are consistent with phase–amplitude coupling (PAC) between theta and gamma oscillations thought
204   to be involved in both working memory and timing (Axmacher et al., 2010; Canolty & Knight,
205   2010; Jensen & Colgin, 2007). Integrate-and-fire attractor networks simulating the lateral
206   entorhinal cortex can produce half-phase oscillatory patterns for coding the seconds to minutes
207   range of time (Rolls & Mills, 2019). Using sequences of firing chains of time cells permits the
208   hippocampus to create time references for memory of elapsed time, which likely applies to
209   retrospective timing (Eichenbaum, 2014; MacDonald et al., 2011, 2014).

210

3. Challenges for Current Interval Timing Models

It is important to note that most of the interval timing models are designed for prospective timing, which has clear onset and offset signals. The biggest challenge for timing models is to make correct predictions for the anatomical, behavioral, and pharmacological evidence (Allman et al., 2014), and for both prospective and retrospective timing (MacDonald et al., 2014).

3.1. Step versus Ramping during Dynamic Acquisition

Animal studies on timing often use the peak-interval procedure, where animals learn to expect food rewards that come after a fixed delay. One typical pattern is that they cluster their responses around the reward time (i.e., peak interval), showing a low–high–low step pattern (Church et al., 1994). Animals initially respond sporadically, then shift to high-rate responses, and set back to low-rate responses after the reward is given during the training or during the probe when the reward is not delivered after a certain long interval. The step pattern suggests that predicting intervals in animals is not a single-shot estimation, rather a target range in which the acquired temporal interval likely occurs. The target range shown in the step-like response profile has two important temporal parameters: response onset ('start') and offset ('stop'). Interestingly, the single-trial analysis of neuronal firing rate in the LIP during decision-making also exhibits discrete 'stepping' dynamics (Latimer et al., 2015, 2016; also see Shadlen et al., 2016). When pooled over all trials, the ensemble averaging mimics the continuous diffusion-to-bound dynamics both in neuronal (Latimer et al., 2015) and behavioral levels (Church et al., 1994). Research shows the acquisition of the onset and offset of the step pattern is asymmetric (Balcı et al., 2009; MacDonald et al., 2012). Animals can quickly learn the temporal criterion and initiate burst responses to the trained temporal criterion during the first several sessions. However, when to stop their responses is acquired separately at a relatively late stage (e.g., Balcı et al., 2009). The separate acquisition of the start and stop time is also supported by the evidence using intracerebral infusions of the protein synthesis inhibitor anisomycin in tracking temporal functionality (MacDonald et al., 2012), in which the differential acquisition of the start and stop times was found to depend on normal functioning in the dorsal striatum (DS) and the ventral striatum (VS), respectively.

The step pattern of responses and the dynamic acquisition of the start and stop signals have two important implications. First, in contrast to the single-shot response models, subjects have sufficient ability to store multiple temporal criteria, as typically assumed by the STT model (Church, 2003; Gibbon et al., 1984), and to judge the difference between the stored time and elapsed

245   time (Gallistel, 1990; Gallistel & Wilkes, 2016; Ward et al., 2012; Wilkes & Gallistel, 2017). To

246   incorporate this, ramping models must consider not a single fixed threshold, but multiple thresholds

247   (e.g., Balcı & Simen, 2014), and the thresholds must be adjustable. The neural oscillator models

248   applying coincidence detection with trial-to-trial scalar variability could, in principle, use a lower

249   coincident activation threshold to capture the step-like responses. The goodness of fit of this

250   approach is yet to be validated. Alternatively, using the ability to store multiple intervals

251   simultaneously, as proposed in the EIO model (Gu et al., 2015), could be another solution to this

252   dynamic acquisition. The second implication of the dynamic acquisition is that the target temporal

253   criterion is acquired quickly, but the reliability of the acquired temporal criterion increases

254   gradually over sessions. Thus, the coefficient of variation (CV), measured by the ratio of the

255   standard deviation to the mean, is not constant during acquisition but approaches a stable value

256   once the steady-state performance is achieved. This poses a challenge to ramping models, which

257   assume the interval and the drift rate have an inverse relation and the drift rate is fixed when the

258   temporal criterion is acquired. It is then a challenge to balance the proportion of the opponent

259   Poisson diffusion process and the excitatory rate such that the CV is decreasing while the interval

260   remains unchanged. Oscillation models (e.g., the SBF model), on the other hand, ascribe a

261   mechanism for possibly detecting the start and stop signal to MSNs within the DS and VS

262   (MacDonald et al., 2012), providing neural networks for this dynamic temporal acquisition. Yet, a

263   quantitative validation of asymmetric acquisition with oscillatory models is needed in future

264   research.

265

266   *3.2. The Onset Problem in Retrospective Timing*

267

268   Both ramping and oscillator models have been first developed specifically for prospective timing,

269   which implicitly assumes an onset to start the ramping process or synchronization of oscillators.

270   For example, the SBF model assumes that the phases of oscillators are reset by a burst of

271   dopaminergic input from the VTA at the beginning of the stimulus onset (Matell & Meck, 2004),

272   and the opDDM starts a ramping process with a bistable switch (Simen et al., 2011). The onset

273   assumption is valid for prospective timing given that the associative learning has already been

274   acquired and subjects know which event is a critical onset event. With the implicit requirement of

275   an onset, both types of models are less applicable to retrospective timing. For example, during an

276   initial phase of the associative learning, multiple sequential events in a trial, such as the subject

277   entering the box and light/sound turning on/off, are potential candidates for subjects to start a timer

278   for predicting the reward (Gallistel, 2003; Gallistel & Wilkes, 2016). Given that onsets and offsets

279 could be many over multiple events (see Fig. 1 for an example), each triggering a ramping process
280 or a coincidence detection process is unrealistic for any neuronal implementations. More likely,
281 instead of using multiple onsets and related ramping or phase-reset processes, subjects may use
282 discrete point events as states to infer critical intervals during associative learning of a target
283 interval. Some researchers suggest that discrete sparse representation of point events likely takes
284 place in episodic memory in the hippocampus (Eichenbaum, 2014, 2017; MacDonald et al., 2014;
285 Rolls & Mills, 2019). Sparse point events coded by phases of oscillators or intrinsic sequential firing
286 chains would be efficient coding schemes for retrospective timing.

287   The onset problem generally exists in associative learning. When a reward follows various
288 event cues, which are often ambiguous in real scenarios, humans and other animals must
289 retrospectively figure out relevant events/intervals that are predictive of critical rewards.
290 Researchers have proposed various models to deal with such ambiguous associative mapping
291 problems (Gallistel & Wilkes, 2016; Namboodiri & Stuber, 2021; Starkweather et al., 2017; Wilkes
292 & Gallistel, 2017). For example, Namboodiri and Stuber (2021) proposed that prospective and
293 retrospective cognitive maps could account for many associative-learning phenomena, such as
294 sudden acquisition of the contingency between a reward predictor and reward. The basic idea of
295 their proposal is that brain circuits store not just the reward value of each state/event, but also the
296 relationships between the various states in the environment in the form of transition probabilities
297 (Starkweather et al., 2017; Sutton & Barto, 2018). Thus, the sequence and relation of states toward
298 a reward can be stored in the form of a successor representation (prospective) and predecessor
299 representation (retrospective) in a cognitive map. Separate storages of prospective and retrospective
300 cognitive maps may seem inefficient and computationally expensive. However, the authors propose
301 efficient neural mechanisms in which the prospective transition probability can be mathematically
302 calculated from the retrospective transition probability based on Bayesian theory.

303
304 *3.3. Computational Accessibility of Encoded Intervals*
305
306 The fact that subjects can acquire the most likely interval among multiple candidate intervals during
307 reinforcement learning has two important implications: (1) multiple retrospective intervals/events
308 must be stored; and (2) those intervals/events must be in a computationally accessible form, a form
309 that permits basic arithmetic computations for the cue competition selection (Gallistel & Gibbon,
310 2000; Gallistel & King, 2009). Researchers have shown such computational ability in temporal cue
311 integration and averaging of multiple intervals (e.g., Aagten-Murphy et al., 2014; De Corte &
312 Matell, 2016a, 2016b; Gu et al., 2016; Matell & Kurti, 2014; Shi & Burr, 2016; Shi et al., 2013)

313 and during the two-step acquisition process for transitioning from one temporal criterion to another

314 (MacDonald et al., 2012; Meck et al., 1984, 2013).

315 In the original STT, the computational accessibility is inherited in the linear accumulation

316 (i.e., pacemaker pulses), such that basic arithmetic computation is possible. However, the model

317 encounters an unbound problem for long intervals, as ensuring a large-enough accumulator is

318 unrealistic for neuronal implementation (Matell & Meck, 2000, 2004). Other ramping models also

319 carry temporal information about elapsed time within the ramping range. However, it is challenging

320 to compare different ramping activities when the ramping rates are different for different target

321 intervals (e.g., opDDM assumes different drift rates for the short and long intervals). Oscillator

322 models with coincidence detection encounter similar challenges with computational accessibility,

323 because the phase patterns of the oscillators are often arbitrary. The brain must then resort to

324 additional resources and processes to compute time differences between multiple intervals. In

325 contrast, multiple-oscillator models (Church & Broadbent, 1990; Gu et al., 2015) could, in

326 principle, preserve the magnitudes of the interval timing and the computational accessibility (e.g.,

327 in log-spacing oscillators).

328

329 ## 4. Integrating Neural Oscillators with Computational Accessibility

330

331 As we briefly reviewed above, by far the most challenges for interval timing models come from

332 dynamic interval acquisition and retrospective timing, where multiple intervals must be stored and

333 compared in a computationally accessible manner. To address this, we first explore possible coding

334 schemes and read-out mechanisms that brains may use.

335

336 *4.1. Neural Oscillators and Internal 'Clocks'*

337

338 Given that intervals and point events (such as onsets and offsets) are two basic forms in associative

339 learning (Gallistel & Wilkes, 2016) and each interval is demarcated by two point events, an efficient

340 encoding scheme would represent one basic form, inferring the other. Note that representing

341 multiple intervals alone does not provide any information about the order of point events. In

342 contrast, encoding point events in a computation-accessible manner makes inference of intervals

343 possible. Moreover, reinforcers are often coupled with critical point events (Killeen & Fetterman,

344 1988; Machado, 1997). Following Occam's principle, encoding point events rather than multiple

345 intervals is likely to minimize the representational complexity (Figure 1). Encoding point events

346 entails a memory process that can accommodate prospective and retrospective timing.

347 Retrospective timing corresponds to the accumulation of evidence for the current event (e.g., time

348 intervals relative to previous point events), namely, updating beliefs about the causes of previous

349 sensory samples, while prospective timing makes predictions about future events (e.g., the current

350 point in time becomes an onset or a predictive cue of a future event). Thus, the point event

351 representation scheme potentially solves the onset problem, as well as serving the state

352 representation with inherited temporal relationships among point events. The brain does not need

353 to initiate multiple ramping or synchronization processes, but simply associates important discrete

354 events with the point representations, better matching the sparse event/object representations in the

355 hippocampus (Rolls & Mills, 2019).

356   In fact, recent studies have shown event-associated temporal activities in the human memory

357 system (Eichenbaum, 2014; Rolls & Mills, 2019; Umbach et al., 2020). For example, time cells fire

358 sequentially at specific points in time (Eichenbaum, 2014; Issa et al., 2020; MacDonald et al., 2011).

359 Similarly, oscillatory patterns in SBF (Matell & Meck, 2000, 2004) and EIO models (Gu et al.,

360 2015) can be treated as coding point events. The pattern shown at a specific time in SBF is

361 determined by the phases of ensemble cortical neurons that oscillate at their endogenous

362 frequencies. Likewise, the EIO model extends oscillations to coupled excitatory–inhibitory

363 oscillation to address the shared oscillatory properties of interval timing and working memory. The

364 excitatory phases of the oscillators can serve as timestamps for point events (Figure 2A). Given that

365 those oscillatory patterns will recur when the interval is long enough (Matell & Meck, 2004), the

366 sequence of oscillatory patterns working as a clock requires multiple long-cycle oscillators.

367 Although not commonly reported, long-cycle oscillatory activities have been shown in the

368 hippocampus neural spikes of anesthetized rats (~11 minutes) (Clement et al., 2008), in calcium

369 signals (Mitra et al., 2018), in EEG signals (Monto et al., 2008), and in the circadian rhythm cells

370 (Green & Gillette, 1982).

371   It is worth noting that the encoding timing in oscillatory phases is not limited to neurons

372 with intrinsic oscillation. A ring attractor network can also generate oscillatory patterns (Fig. 2B),

373 in which neurons are functionally arranged on a ring with a rotation-invariant connectivity

374 (Boucheny et al., 2005; Popovych et al., 2011; Seeholzer et al., 2017; York & van Rossum, 2009).

375 With strong recurrent connections and appropriate adjustment of connection weights, such a ring

376 attractor model can generate self-sustained firing activities at a specific location ('bump' state).

377 Some have suggested the ring network as the working memory representation of physical

378 magnitudes, such as spatial orientation, angular position, and head direction (Dieterich et al., 2018;

379 Seeholzer et al., 2017; York & van Rossum, 2009; Zhang, 1996). When two or more rings are

380 appropriately combined (Xie et al., 2002; Zhang, 1996), constant external input to the rings can

381   generate a moving-bump state, that is, an oscillation that depends on the strength of the input.

382   Similar computational circuits may also serve as the basis of self-generated sequences of neuronal

383   firing patterns in the hippocampus, entorhinal, prefrontal, and parietal cortex that exhibit oscillatory

384   characteristics (Buzsáki & Llinás, 2017; Pastalkova et al., 2008; Rolls & Mills, 2019; Tsao et al.,

385   2018). For example, opponent ramping cells in the lateral entorhinal cortex can be simulated as an

386   integrate-and-fire attractor network to generate EIOs (Rolls & Mills, 2019), similar to the EIO

387   model (Gu et al., 2015).

388

389   *4.2. Oscillatory Patterns with Computational Accessibility*

390

391   Although all oscillatory patterns could, in principle, represent point events, the efficacy of read-out

392   of the order relation between events varies dramatically among different models. Most oscillatory

393   models do not specify how oscillatory patterns should be stored for the temporal-order relation. The

394   EIO model (Gu et al., 2015), though not explicitly mentioning the patterns for the order of point

395   events, uses a set of different frequencies of oscillators, similar to the multi-oscillator model

396   (Church & Broadbent, 1990). The pattern based on multifrequency oscillators has a potential ability

397   to encode the order of temporal events. The ring attractor network, on the other hand, has implicit

398   sequential coding for the order of events. Note that individual oscillatory patterns can only represent

399   a limited range of time intervals. When the interval exceeds the range, it begs for additional

400   oscillatory sequences with lower frequencies or ring attractor networks with slow propagation

401   speed. Thus, in principle, a combination of multifrequency oscillators or different sizes of ring

402   attractors (Navratilova et al., 2012) can represent a wide range of temporal events. Those oscillators

403   can be distributed across the network of different neuronal regions (Ivry & Schlerf, 2008; Ivry &

404   Spencer, 2004).

405   Yet, we must consider another key signature in the selection of oscillatory patterns — the

406   scalar property. The scalar property naturally leads to the Weber–Fechner law (Fechner, 1860).

407   That is, the internal representation of the external magnitudes is likely on a logarithmic scale. The

408   logarithmic scale of representation is regarded as a natural result of a set of optimized sensors to

409   minimize a relative error measure (Portugal & Svaiter, 2010; Sun et al., 2012) for an uncertain

410   world (Howard, 2018; Howard & Shankar, 2018). It is interesting to note that our numerical

411   notation system exactly uses the logarithmic coding. For example, magnitudes within 1000 require

412   only three digits, each with 10 states. The grid cell system in the entorhinal cortex (see Moser et al.,

413   2008 for a review) uses a very similar scheme to provide a metric for two-dimensional space and

414   is an example of spatially periodic coding. The grid cell system is thought to consist of toroidal

415   attractor networks that are driven by running speed. Different 'grids' with increasing spacing are

416   organized along the entorhinal cortex, with each grid representing a range of distances, like one

417   digit of a multidigit mileage counter, or like the periods in a multi-oscillator system. Similarly, the

418   logarithmic coding scheme can be realized by using log-spacing oscillators with a half-phase coding

419   scheme, such as EIO oscillators (Gu et al., 2015) or opponent ramping processes in an attractor

420   network (Rolls & Mills, 2019). It should be noted that each half-phase of a given frequency is coded

421   by the active 'on' states of the opponent oscillators (see dashed vs solid lines in Fig. 2). The read-

422   out of the two oscillatory phases can be regarded as a chain of combinatorial binary symbols (see

423   Figs 2A and 3A).

424   The fact that time cells in the hippocampus fire at a specific moment in time led researchers

425   to suggest that time cells are essential for discrete time stamping and binding sequential events in

426   memory (Eichenbaum, 2014; Issa et al., 2020; MacDonald et al., 2011; Rolls & Mills, 2019). To

427   efficiently store those read-out combinatory nodes from the multifrequency oscillators, here we

428   propose that those redundant nodes (mainly from low-frequency EIOs based on their similarity in

429   population coding) are shared across events. Specifically, codes from the read-out that do not differ

430   from the preceding codes in the low-frequency phases will share the same memory representation

431   (see illustration in Fig. 3B line connections). Such shared representation has an additional benefit

432   — robust against noise perturbation. Even when some noise corrupts the shared nodes of two

433   adjacent events, the temporal relation between two events remains intact. Such robust memory of

434   the temporal vicinity also occurs in our daily life. For example, you may not correctly remember

435   which day you had a conversation with your friend A before visiting your friend B, but you still

436   remember the temporal relation between events A and B.

437   Unlike other arbitrary oscillatory patterns, calculating time intervals between any two stored

438   events is relatively easy for the log-spacing combinatorial codes. The realization could be first

439   comparing correspondent nodes of the same frequencies from two events, then summing up their

440   represented time intervals together:

441
$$T = k \sum_{i=1}^{n} \frac{S_i^{(2)} - S_i^{(1)}}{f_i}$$

442   where $\{S_i^{(1)}, i = 1, ... \ n\}$ and $\{S_i^{(2)}, i = 1, ... \ n\}$ are two combinatorial codes, and $\{f_i, i = 1, ..., n\}$

443   their corresponding frequencies. k denotes a normalization coefficient.

444   One interesting outcome of such interval computation with the shared representation is that

445   those shared nodes (low frequencies), corrupted or not, do not influence the interval estimation.

446   Thus, intervals with the same length should be equally precise, independent of their location in the

447   sequence, as long as the memory decay is negligible. However, short relative to long intervals have

448   fewer independent nodes that are subjected to noise perturbation and global nuisance correlations.

449   Given that the number of independent nodes is proportional to the log-scale of the represented

450   intervals, the noise perturbation and/or global nuisance correlation to the independent nodes would

451   naturally lead to the scalar property.

452

453   ## 5. Prospective and Retrospective Timing

454

455   The multifrequency oscillators with discrete time stamping in memory are suitable for both

456   prospective and retrospective timing. Time stamping for discrete sequential events in memory

457   (Eichenbaum, 2014; Issa et al., 2020; MacDonald et al., 2011; Rolls & Mills, 2019) could

458   potentially solve the onset problems encountered by those prospective timing models. Representing

459   all events in memory also enables the brain to learn to time (Killeen & Fetterman, 1988; Machado,

460   1997) and discriminate the critical interval from other intervals (Gallistel & Wilkes, 2016; Wilkes

461   & Gallistel, 2017). Using the multifrequency oscillatory patterns as time stamping also preserves

462   the temporal relationships among critical states/events, which enables efficient calculation of the

463   predecessor representation in a retrospective cognitive map (the distance from a reward state to any

464   predecessor event is computationally accessible through the event timestamps). In addition, the

465   sparse shared representation of the combinatorial codes boosts the efficiency of memory usage and

466   keeps the sequential structure of the events. The scalar property observed in behavioral results

467   (Gibbon, 1977; Gibbon et al., 1984; Simen et al., 2013) is thus due to this shared representation of

468   time events in memory. One prediction of this shared representation is that the number of

469   independent nodes will increase proportionally to the number of events, which would eventually

470   reduce the precision of the representation, considering limited memory resources. In other words,

471   the observed Weber fraction may depend on the number of events within a given interval.

472   One critical feature of prospective time is that we have a continuous sense of the passage of

473   time. This is a natural outcome from the accumulator in ramping models (e.g., Gibbon et al., 1984;

474   Simen et al., 2011), while it is lacking in oscillatory models (Matell & Meck, 2000, 2004; Oprisan

475   & Buhusi, 2011). The model of multifrequency oscillators with computational accessibility,

476   however, preserves the continuous sense of time through computation. The flow of time is a

477   continuous calculation of the timestamp of 'now' to preceding critical events, forming a sequence

478   of intervals. It is also possible that the continuous sense of time comes directly from the ramping

479   cells embedded in the attractor neural networks in the oscillatory system (Issa et al., 2020; Rolls &

480 Mills, 2019). Furthermore, despite a periodic multilayer representation of space in the entorhinal
481 cortex (Moser et al., 2014), our sense of distance and position in the horizontal plane is continuous.
482

6. Concluding Remarks

484

485 It is a challenge to develop neurobiological plausible models to account for multifaceted aspects of
486 interval timing. The stochastic ramping, the neural oscillator and time cells provide possible neural
487 implementations of the prospective timing and some of them incorporate the scalar property of the
488 interval timing. Those models, however, lack computational accessibility for retrospective timing.
489 Here, we propose a conceptual model with multifrequency oscillators, extended from the EIO
490 model, to incorporate computational accessibility, suitable for both prospective and retrospective
491 timing. The model assumes that the event read-out phase patterns from the multisensory oscillators
492 are stored in a shared memory and intervals are calculated based on the represented combinatorial
493 nodes, with the shared representation potentially causing the scalar property. It should be noted that
494 making this conceptual model biologically feasible, several challenges remain to be solved. For
495 example, the multi-oscillator coding scheme requires slow cycle oscillators for minutes and hours
496 in neural spikes, which are relatively rare (except the circadian rhythmic cells). It also remains
497 unclear concerning neural circuits of interval computation between two oscillatory patterns.
498 Nevertheless, our model provides a feasible way to incorporate both retrospective and prospective
499 timing.

500

References

502

503 Aagten-Murphy, D., Iversen, J. R., Williams, C. L., & Meck, W. H. (2014). Novel inversions in auditory sequences
504   provide evidence for spontaneous subtraction of time and number. *Timing Time Percept.*, *2*, 188–209. doi:
505   10.1163/22134468-00002028
506 Addyman, C., French, R. M., & Thomas, E. (2016). Computational models of interval timing. *Curr. Opin. Behav.*
507   *Sci.*, *8*, 140–146. https://doi.org/10.1016/j.cobeha.2016.01.004
508 Allman, M. J., & Meck, W. H. (2012). Pathophysiological distortions in time perception and timed performance. In
509   *Brain*, *135*, 656–677. https://doi.org/10.1093/brain/awr210
510 Allman, M. J., Teki, S., Griffiths, T. D., & Meck, W. H. (2014). Properties of the internal clock : first- and second-
511   order principles of subjective time. *Annu. Rev. Psychol.*, *65*, 743–771. doi: 10.1146/annurev-psych-010213-
512   115117
513 Allman, M. J., Penney, T. B., & Meck, W. H. (2016). A Brief History of " The Psychology of Time Perception".
514   *Timing Time Percept.*, *4*, 299–314. https://doi.org/10.1163/22134468-00002071
515 Axmacher, N., Henseler, M. M., Jensen, O., Weinreich, I., Elger, C. E., & Fell, J. (2010). Cross-frequency coupling

516   supports multi-item working memory in the human hippocampus. *Proc. Natl Acad. Sci. U. S. A.*, *107*, 3228–
517   3233. doi: 10.1073/pnas.0911531107

518 Balcı, F., & Simen, P. (2014). Decision processes in temporal discrimination. *Acta Psychol.*, *149*, 157–168.
519   https://doi.org/10.1016/j.actpsy.2014.03.005

520 Balcı, F., Gallistel, C. R., Allen, B. D., Frank, K. M., Gibson, J. M., & Brunner, D. (2009). Acquisition of peak
521   responding: what is learned? *Behav. Processes*, *80*, 67–75. https://doi.org/10.1016/j.beproc.2008.09.010

522 Beck, J. M., Ma, W. J., Pitkow, X., Latham, P. E., & Pouget, A. (2012). Not noisy, just wrong: the role of suboptimal
523   inference in behavioral variability. *Neuron*, *74*, 30–39. https://doi.org/10.1016/j.neuron.2012.03.016

524 Boucheny, C., Brunel, N., & Arleo, A. (2005). A continuous attractor network model without recurrent excitation:
525   maintenance and integration in the head direction cell system. *J. Comput. Neurosci.*, *18*, 205–227.
526   https://doi.org/10.1007/s10827-005-6559-y

527 Buhusi, C. V., & Meck, W. H. (2005). What makes us tick? Functional and neural mechanisms of interval timing.
528   *Nat. Rev. Neurosci.*, *6*, 755–765. https://doi.org/10.1038/nrn1764

529 Buhusi, C. V., & Oprisan, S. A. (2013). Time-scale invariance as an emergent property in a perceptron with realistic,
530   noisy neurons. *Behav. Processes*, *95*, 60–70. https://doi.org/10.1016/j.beproc.2013.02.015

531 Buonomano, D. V. (2000). Decoding temporal information: a model based on short-term synaptic plasticity. *J.*
532   *Neurosci.*, *20*, 1129–1141. https://doi.org/10.1523/JNEUROSCI.20-03-01129.2000

533 Buzsáki, G., & Llinás, R. (2017). Space and time in the brain. *Science*, *358*, 482–485. doi: 10.1126/science.aan8869

534 Canolty, R. T., & Knight, R. T. (2010). The functional role of cross-frequency coupling. *Trends Cogn. Sci.*, *14*, 506–
535   515. https://doi.org/10.1016/j.tics.2010.09.001

536 Chen, S., Shi, Z., Müller, H. J., & Geyer, T. (2021). Multisensory visuo-tactile context learning enhances the
537   guidance of unisensory visual search. *Sci. Rep.*, *11*, 9439. https://doi.org/10.1038/s41598-021-88946-6

538 Church, R. M. (2003). A concise introduction to scalar timing theory. In W. H. Meck (Ed.), *Functional and Neural*
539   *Mechanisms of Interval Timing* (pp. 1–22). Boca Raton, FA, USA: CRC Press.
540   https://doi.org/10.1201/9780203009574.sec1

541 Church, R. M., & Broadbent, H. A. (1990). Alternative representations of time, number, and rate. *Cognition*, *37*, 55–
542   81. https://doi.org/10.1016/0010-0277(90)90018-F

543 Church, R. M., Meck, W. H., & Gibbon, J. (1994). Application of scalar timing theory to individual trials. *J. Exp.*
544   *Psychol. Anim. Behav. Process., 20*, 135–155. doi: 10.1037//0097-7403.20.2.135

545 Clement, E. A., Richard, A., Thwaites, M., Ailon, J., Peters, S., & Dickson, C. T. (2008). Cyclic and sleep-like
546   spontaneous alternations of brain state under urethane anaesthesia. *PloS ONE*, *3*, e2004.
547   https://doi.org/10.1371/journal.pone.0002004

548 Coull, J. T., Cheng, R.-K., & Meck, W. H. (2010). Neuroanatomical and neurochemical substrates of timing.
549   *Neuropsychopharmacology*, *36*, 3–25. https://doi.org/10.1038/npp.2010.113

550 De Corte, B. J., & Matell, M. S. (2016a). Temporal averaging across multiple response options: insight into the
551   mechanisms underlying integration. *Anim. Cogn.*, *19*, 329–342. https://doi.org/10.1007/s10071-015-0935-4

552 De Corte, B. J., & Matell, M. S. (2016b). Interval timing, temporal averaging, and cue integration. *Curr. Opin.*
553   *Behav. Sci.*, *8*, 60–66. https://doi.org/10.1016/j.cobeha.2016.02.004

554 Dieterich, M., Glasauer, S., & Brandt, T. (2018). Why acute unilateral vestibular midbrain lesions rarely manifest
555   with rotational vertigo: a clinical and modelling approach to head direction cell function. *J. Neurol.*, *265*, 1184–
556   1198. https://doi.org/10.1007/s00415-018-8828-5

557 Eichenbaum, H. (2014). Time cells in the hippocampus: a new dimension for mapping memories. *Nat. Rev.*
558   *Neurosci.*, *15*, 732–744. https://doi.org/10.1038/nrn3827

559 Eichenbaum, H. (2017). On the integration of space, time, and memory. *Neuron*, *95*, 1007–1018.
560   https://doi.org/10.1016/j.neuron.2017.06.036

561 Fechner, G. T. (1860). *Elemente der Psychophysik*. Leipzig, Germany: Breitkopf und Härtel.

562 Frankland, P. W., & Bontempi, B. (2005). The organization of recent and remote memories. *Nat. Rev. Neurosci.*, *6*,
563   119–130. https://doi.org/10.1038/nrn1607

564 Friston, K., & Buzsáki, G. (2016). The functional anatomy of time: what and when in the brain. *Trends Cogn. Sci.*,
565   *20*, 500–511. https://doi.org/10.1016/j.tics.2016.05.001

566 Gallistel, C. R. (1990). *The organization of learning*. Cambridge, MA, USA: MIT Press.

567 Gallistel, C. R. (2003). Conditioning from an information processing perspective. *Behav. Processes*, *62*, 89–101.
568   https://doi.org/10.1016/S0376-6357(03)00019-6

569 Gallistel, C. R., & Gibbon, J. (2000). Time, rate, and conditioning. *Psychol. Rev.*, *107*, 289–344.
570   https://doi.org/10.1037/0033-295X.107.2.289

571 Gallistel, C. R., & King, A. P. (2009). *Memory and the Computational Brain*. Chichester, UK: Wiley-Blackwell.

572 Gallistel, C. R., & Wilkes, J. T. (2016). Minimum description length model selection in associative learning. *Curr.*
573   *Opin. Behav. Sci.*, *11*, 8–13. https://doi.org/10.1016/j.cobeha.2016.02.025

574 Gibbon, J. (1977). Scalar expectancy theory and Weber's law in animal timing. *Psychol. Rev.*, *84*, 279–325.
575   https://doi.org/10.1037/0033-295X.84.3.279

576 Gibbon, J. (1992). Ubiquity of scalar timing with a Poisson clock. *J. Math. Psychol.*, *36*, 283–293.
577   https://doi.org/10.1016/0022-2496(92)90041-5

578 Gibbon, J., Church, R. M., & Meck, W. H. (1984). Scalar timing in memory. *Ann. N. Y. Acad. Sci.*, *423*, 52–77.
579   https://doi.org/10.1111/j.1749-6632.1984.tb23417.x

580 Goel, A., & Buonomano, D. V. (2014). Timing as an intrinsic property of neural networks: evidence from *in vivo* and
581   *in vitro* experiments. *Philos. Trans. R. Soc. Lond. B Biol. Sci.*, *369*, 20120460. doi: 10.1098/rstb.2012.0460

582 Green, D. J., & Gillette, R. (1982). Circadian rhythm of firing rate recorded from single cells in the rat
583   suprachiasmatic brain slice. *Brain Res.*, *245*, 198–200. https://doi.org/10.1016/0006-8993(82)90361-4

584 Grossberg, S., & Merrill, J. W. L. (1992). A neural network model of adaptively timed reinforcement learning and
585   hippocampal dynamics. *Cogn. Brain Res.*, *1*, 3–38. https://doi.org/10.1016/0926-6410(92)90003-A

586 Grossberg, S., & Merrill, J. W. L. (1996). The hippocampus and cerebellum in adaptively timed learning, recognition,
587   and movement. *J. Cogn. Neurosci.*, *8*, 257–277. https://doi.org/10.1162/jocn.1996.8.3.257

588 Grossberg, S., & Schmajuk, N. A. (1989). Neural dynamics of adaptive timing and temporal discrimination during
589   associative learning. *Neural Netw.*, *2*, 79–102. https://doi.org/10.1016/0893-6080(89)90026-9

590 Gu, B.-M., van Rijn, H., & Meck, W. H. (2015). Oscillatory multiplexing of neural population codes for interval
591   timing and working memory. *Neurosci. Biobehav. Rev.*, *48*, 160–185.
592   https://doi.org/10.1016/j.neubiorev.2014.10.008

593 Gu, B.-M., Jurkowski, A. J., Shi, Z., & Meck, W. H. (2016). Bayesian optimization of interval timing and biases in
594   temporal memory as a function of temporal context, feedback, and dopamine levels in young, aged and
595   Parkinson's disease patients. *Timing Time Percept.*, *4*, 315–342. https://doi.org/10.1163/22134468-00002072

596 Hardy, N. F., & Buonomano, D. V. (2016). Neurocomputational models of interval and pattern timing. *Curr. Opin.*
597   *Behav. Sci.*, *8*, 1–8. https://doi.org/10.1016/j.cobeha.2016.01.012

598 Hass, J., & Durstewitz, D. (2016). Time at the center, or time at the side? Assessing current models of time

599   perception. *Curr. Opin. Behav. Sci.*, *8*, 238–244. https://doi.org/10.1016/j.cobeha.2016.02.030

600 Howard, M. W. (2018). Memory as perception of the past: compressed time inmind and brain. *Trends Cogn. Sci.*, *22*,

601   124–136. https://doi.org/10.1016/j.tics.2017.11.004

602 Howard, M. W., & Shankar, K. H. (2018). Neural scaling laws for an uncertain world. *Psychol. Rev.*, *125*, 47–58. doi:

603   10.1037/rev0000081

604 Issa, J. B., Tocker, G., Hasselmo, M. E., Heys, J. G., & Dombeck, D. A. (2020). Navigating through time: A spatial

605   navigation perspective on how the brain may encode time. *Annu. Rev. Neurosci.*, *43*, 73–93. 10.1146/annurev-

606   neuro-101419-011117

607 Ivry, R. B., & Schlerf, J. E. (2008). Dedicated and intrinsic models of time perception. In *Trends Cogn. Sci.*, *12*, 273–

608   280). https://doi.org/10.1016/j.tics.2008.04.002

609 Ivry, R. B., & Spencer, R. M. C. (2004). The neural representation of time. *Curr. Opin. Neurobiol.*, *14*, 225–232.

610   https://doi.org/10.1016/j.conb.2004.03.013

611 Jazayeri, M., & Shadlen, M. N. (2015). A neural mechanism for sensing and reproducing a time interval. *Curr. Biol.*,

612   *25*, 2599–2609. https://doi.org/10.1016/j.cub.2015.08.038

613 Jensen, O., & Colgin, L. L. (2007). Cross-frequency coupling between neuronal oscillations. *Trends Cogn. Sci.*, *11*,

614   267–269. https://doi.org/10.1016/j.tics.2007.05.003

615 Killeen, P. R., & Fetterman, J. G. (1988). A behavioral theory of timing. *Psychol. Rev.*, *95*, 274–295.

616   https://doi.org/10.1037/0033-295X.95.2.274

617 Latimer, K. W., Yates, J. L., Meister, M. L. R., Huk, A. C., & Pillow, J. W. (2015). Single-trial spike trains in parietal

618   cortex reveal discrete steps during decision-making. *Science*, *349*, 184–187. doi: 10.1126/science.aaa40

619 Latimer, K. W., Yates, J. L., Meister, M. L. R., Huk, A. C., & Pillow, J. W. (2016). Response to Comment on

620   "Single-trial spike trains in parietal cortex reveal discrete steps during decision-making". *Science*, *351*, 1406.

621   doi: 10.1126/science.aad359

622 Lusk, N. A., Petter, E. A., MacDonald, C. J., & Meck, W. H. (2016). Cerebellar, hippocampal, and striatal time cells.

623   *Curr. Opin. Behav. Sci.*, *8*, 186–192. https://doi.org/10.1016/j.cobeha.2016.02.020

624 Luzardo, A., Alonso, E., & Mondragón, E. (2017). A Rescorla-Wagner drift-diffusion model of conditioning and

625   timing, PLoS Comput. Biol., *13*, e1005796. https://doi.org/10.1371/journal.pcbi.1005796

626 MacDonald, C. J., Lepage, K. Q., Eden, U. T., & Eichenbaum, H. (2011). Hippocampal "time cells" bridge the gap in

627   memory for discontiguous events. *Neuron*, *71*, 737–749. https://doi.org/10.1016/j.neuron.2011.07.012

628 MacDonald, C. J., Cheng, R.-K., & Meck, W. H. (2012). Acquisition of "Start" and "Stop" response thresholds in

629   peak-interval timing is differentially sensitive to protein synthesis inhibition in the dorsal and ventral striatum.

630   *Front. Integr. Neurosci.*, *6*, 10. https://doi.org/10.3389/fnint.2012.00010

631 MacDonald, C. J., Fortin, N. J., Sakata, S., & Meck, W. H. (2014). Retrospective and prospective views on the role of

632   the hippocampus in interval timing and memory for elapsed time. *Timing Time Percept.*, *2*, 51–61.

633   https://doi.org/10.1163/22134468-00002020

634 Machado, A. (1997). Learning the temporal dynamics of behavior. *Psychol. Rev.*, *104*, 241–265.

635   https://doi.org/10.1037/0033-295X.104.2.241

636 Matell, M. S., & Kurti, A. N. (2014). Reinforcement probability modulates temporal memory selection and

637   integration processes. *Acta Psychol.*, *147*, 80–91. https://doi.org/10.1016/j.actpsy.2013.06.006

638 Matell, M. S., & Meck, W. H. (2000). Neuropsychological mechanisms of interval timing behavior. *BioEssays*, *22*,

639   94–103. https://doi.org/10.1002/(SICI)1521-1878(200001)22:1<94::AID-BIES14>3.0.CO;2-E

640 Matell, M. S., & Meck, W. H. (2004). Cortico-striatal circuits and interval timing: coincidence detection of

641   oscillatory processes. *Cogn. Brain Res.*, *21*, 139–170. https://doi.org/10.1016/j.cogbrainres.2004.06.012

642 Matthews, W. J., & Meck, W. H. (2016). Temporal cognition: connecting subjective time to perception, attention,

643   and memory. *Psychol. Bull.*, *142*, 865–907. https://doi.org/10.1037/bul0000045

644 Meck, W. H. (1983). Selective adjustment of the speed of internal clock and memory processes. *J. Exp. Psychol.*

645   *Anim. Behav. Process., 9*, 171–201. https://doi.org/10.1037/0097-7403.9.2.171

646 Meck, W. H., Komeily-Zadeh, F. N., & Church, R. M. (1984). Two-step acquisition: Modification of an internal

647   clock's criterion. *J. Exp. Psychol. Anim. Behav. Process.*, *10*, 297–306. https://doi.org/10.1037/0097-

648   7403.10.3.297

649 Meck, W. H., Church, R. M., & Matell, M. S. (2013). Hippocampus, time, and memory–A retrospective analysis.

650   *Behav. Neurosci.*, *127*, 642–654. https://doi.org/10.1037/a0034201

651 Merchant, H., Zarco, W., & Prado, L. (2008). Do we have a common mechanism for measuring time in the hundreds

652   of millisecond range? Evidence from multiple-interval timing tasks. *J. Neurophysiol.*, *99*, 939–949.

653   https://doi.org/10.1152/jn.01225.2007

654 Merchant, H., Harrington, D. L., & Meck, W. H. (2013). Neural basis of the perception and estimation of time. *Annu.*

655   *Rev. Neurosci.*, *36*, 313–336. https://doi.org/10.1146/annurev-neuro-062012-170349

656 Mitra, A., Kraft, A., Wright, P., Acland, B., Snyder, A. Z., Rosenthal, Z., Czerniewski, L., Bauer, A., Snyder, L.,

657   Culver, J., Lee, J.-M., & Raichle, M. E. (2018). Spontaneous infra-slow brain activity has unique spatiotemporal

658   dynamics and laminar structure. *Neuron*, *98*, 297–305.e6. https://doi.org/10.1016/j.neuron.2018.03.015

659 Monto, S., Palva, S., Voipio, J., & Palva, J. M. (2008). Very slow EEG fluctuations predict the dynamics of stimulus

660   detection and oscillation amplitudes in humans. *J. Neurosci.*, *28*, 8268–8272.

661   https://doi.org/10.1523/JNEUROSCI.1910-08.2008

662 Moser, E. I., Kropff, E., & Moser, M.-B. (2008). Place cells, grid cells, and the brain's spatial representation system.

663   *Annu. Rev. Neurosci.*, *31*, 69–89. doi: 10.1146/annurev.neuro.31.061307.090723

664 Moser, E. I., Roudi, Y., Witter, M. P., Kentros, C., Bonhoeffer, T., & Moser, M.-B. (2014). Grid cells and cortical

665   representation. *Nat. Rev. Neurosci.*, *15*, 466–481. https://doi.org/10.1038/nrn3766

666 Namboodiri, V. M. K., & Stuber, G. D. (2021). The learning of prospective and retrospective cognitive maps within

667   neural circuits. *Neuron*, *109*, 3552–3575. https://doi.org/10.1016/j.neuron.2021.09.034

668 Narayanan, N. S. (2016). Ramping activity is a cortical mechanism of temporal control of action. *Curr. Opin. Behav.*

669   *Sci.*, *8*, 226–230. https://doi.org/10.1016/j.cobeha.2016.02.017

670 Navratilova, Z., Giocomo, L. M., Fellous, J.-M., Hasselmo, M. E., & McNaughton, B. L. (2012). Phase precession

671   and variable spatial scaling in a periodic attractor map model of medial entorhinal grid cells with realistic after-

672   spike dynamics. *Hippocampus*, *22*, 772–789. https://doi.org/10.1002/hipo.20939

673 Oprisan, S. A., & Buhusi, C. V. (2011). Modeling pharmacological clock and memory patterns of interval timing in a

674   striatal beat-frequency model with realistic, noisy neurons. *Front. Integr. Neurosci.*, *5*, 52. doi:

675   10.3389/fnint.2011.00052

676 Parker, K. L., Chen, K.-H., Kingyon, J. R., Cavanagh, J. F., & Narayanan, N. S. (2014). D_1-dependent 4 Hz

677   oscillations and ramping activity in rodent medial frontal cortex during interval timing. *J. Neurosci.*, *34*, 16774–

678   16783. https://doi.org/10.1523/JNEUROSCI.2772-14.2014

679 Pastalkova, E., Itskov, V., Amarasingham, A., & Buzsáki, G. (2008). Internally generated cell assembly sequences in

680   the rat hippocampus. *Science*, *321*, 1322–1327. doi: 10.1126/science.1159775

681   Popovych, O. V., Yanchuk, S., & Tass, P. A. (2011). Delay- and coupling-induced firing patterns in oscillatory neural

682   loops. *Phys. Rev. Lett.*, *107*, 228102. https://doi.org/10.1103/PhysRevLett.107.228102

683   Portugal, R. D., & Svaiter, B. F. (2010). Weber-Fechner law and the optimality of the logarithmic scale. *Minds Mach.*

684   *(Dordr.)*, *21*, 73–81. https://doi.org/10.1007/s11023-010-9221-z

685   Ratcliff, R., Cherian, A., & Segraves, M. (2003). A comparison of macaque behavior and superior colliculus neuronal

686   activity to predictions from models of two-choice decisions. *J. Neurophysiol.*, *90*, 1392–1407.

687   https://doi.org/10.1152/jn.01049.2002

688   Rolls, E. T., & Mills, P. (2019). The generation of time in the hippocampal memory system. *Cell Rep.*, *28*, 1649–

689   1658.e6. https://doi.org/10.1016/j.celrep.2019.07.042

690   Seeholzer, A., Deger, M., & Gerstner, W. (2017). Efficient low-dimensional approximation of continuous attractor

691   networks. In arXiv:1711.08032 [q-bio.NC]. https://doi.org/10.48550/arXiv.1711.08032

692   Shadlen, M. N., Kiani, R., Newsome, W. T., Gold, J. I., Wolpert, D. M., Zylberberg, A., Ditterich, J., de Lafuente, V.,

693   Yang, T., & Roitman, J. (2016). Comment on "Single-trial spike trains in parietal cortex reveal discrete steps

694   during decision-making". *Science*, *351*, 1406. https://doi.org/10.1126/science.aad3242

695   Shi, Z., & Burr, D. (2016). Predictive coding of multisensory timing. *Curr. Opin. Behav. Sci.*, *8*, 200–206.

696   https://doi.org/10.1016/j.cobeha.2016.02.014

697   Shi, Z., Church, R. M., & Meck, W. H. (2013). Bayesian optimization of time perception. *Trends Cogn. Sci.*, *17*,

698   556–564. https://doi.org/10.1016/j.tics.2013.09.009

699   Simen, P., Balci, F., deSouza, L., Cohen, J. D., & Holmes, P. (2011). A model of interval timing by neural

700   integration. *J. Neurosci.*, *31*, 9238–9253. https://doi.org/10.1523/JNEUROSCI.3121-10.2011

701   Simen, P., Rivest, F., Ludwig, E. A., Balci, F., & Killeen, P. (2013). Timescale invariance in the pacemaker-

702   accumulator family of timing models. *Timing Time Percept.*, *1*, 159–188. https://doi.org/10.1163/22134468-

703   00002018

704   Simen, P., Vlasov, K., & Papadakis, S. (2016). Scale (in)variance in a unified diffusion model of decision making and

705   timing. *Psychol. Rev.*, *123*, 151–181. https://doi.org/10.1037/rev0000014

706   Starkweather, C. K., Babayan, B. M., Uchida, N., & Gershman, S. J. (2017). Dopamine reward prediction errors

707   reflect hidden-state inference across time. *Nat. Neurosci.*, *20*, 581–589. https://doi.org/10.1038/nn.4520

708   Sun, J. Z., Wang, G. I., Goyal, V. K., & Varshney, L. R. (2012). A framework for Bayesian optimality of

709   psychophysical laws. *J. Math. Psychol.*, *56*, 495–501. https://doi.org/10.1016/j.jmp.2012.08.002

710   Sutton, R. S., & Barto, A. G. (2018). *Reinforcement learning*: *An Introduction* (2nd ed). Cambridge, MA, USA: MIT

711   Press.

712   Tsao, A., Sugar, J., Lu, L., Wang, C., Knierim, J. J., Moser, M.-B., & Moser, E. I. (2018). Integrating time from

713   experience in the lateral entorhinal cortex. *Nature*, *561*, 57–62. https://doi.org/10.1038/s41586-018-0459-6

714   Umbach, G., Kantak, P., Jacobs, J., Kahana, M., Pfeiffer, B. E., Sperling, M., & Lega, B. (2020). Time cells in the

715   human hippocampus and entorhinal cortex support episodic memory. *Proc. Natl Acad. Sci. U. S. A.*, *117*,

716   28463–28474. https://doi.org/10.1073/pnas.2013250117

717   Ward, R. D., Gallistel, C. R., Jensen, G., Richards, V. L., Fairhurst, S., & Balsam, P. D. (2012). Conditioned stimulus

718   informativeness governs conditioned stimulus−unconditioned stimulus associability. *J. Exp. Psychol. Anim.*

719   *Behav. Process.*, *38*, 217–232. https://doi.org/10.1037/a0027621

720   Wilkes, J. T., & Gallistel, C. R. (2017). Information theory, memory, prediction, and timing in associative learning.

721   In A. A. Moustafa (Ed.), *Computational models of brain and behavior* (pp. 481–492). Chichester, UK: Wiley-
722   Blackwell. https://doi.org/10.1002/9781119159193.ch35

723 Wittmann, M., Simmons, A. N., Aron, J. L., & Paulus, M. P. (2010). Accumulation of neural activity in the posterior
724   insula encodes the passage of time. *Neuropsychologia*, *48*, 3110–3120.
725   https://doi.org/10.1016/j.neuropsychologia.2010.06.023

726 Xie, X., Hahnloser, R. H. R., & Seung, H. S. (2002). Double-ring network model of the head-direction system. *Phys.*
727   *Rev. E, Stat. Nonlin. Soft Matter Phys.*, *66*, 041902. doi: 10.1103/PhysRevE.66.041902

728 York, L. C., & van Rossum, M. C. W. (2009). Recurrent networks with short term synaptic depression. *J. Comput.*
729   *Neurosci.*, *27*, 607. https://doi.org/10.1007/s10827-009-0172-4

730 Zhang, K. (1996). Representation of spatial orientation by the intrinsic dynamics of the head-direction cell ensemble:
731   a theory. *J. Neurosci.*, *16*, 2112–2126. https://doi.org/10.1523/JNEUROSCI.16-06-02112.1996

732
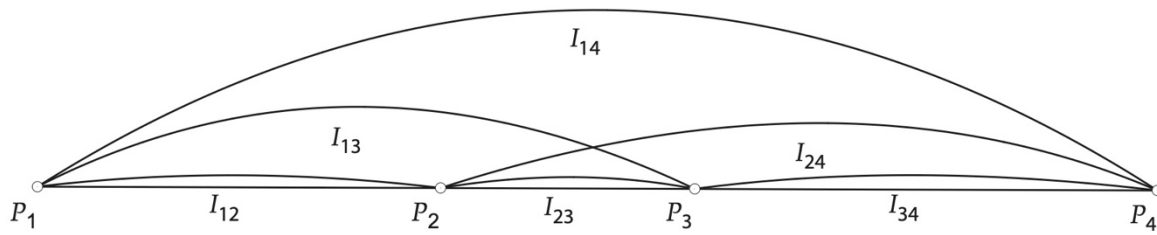
733
734   **Figure 1.** Illustration of the onset problem. Often there are multiple events and multiple intervals. For example, four
735   consecutive point events (P_1, P_2, P_3, P_4) can construct six different intervals $\{I_{ij}\}$. The construction power of point events
736   and intervals is asymmetric. The point events can fully determine the intervals, whereas the intervals cannot determine
737   the order of point events.
738
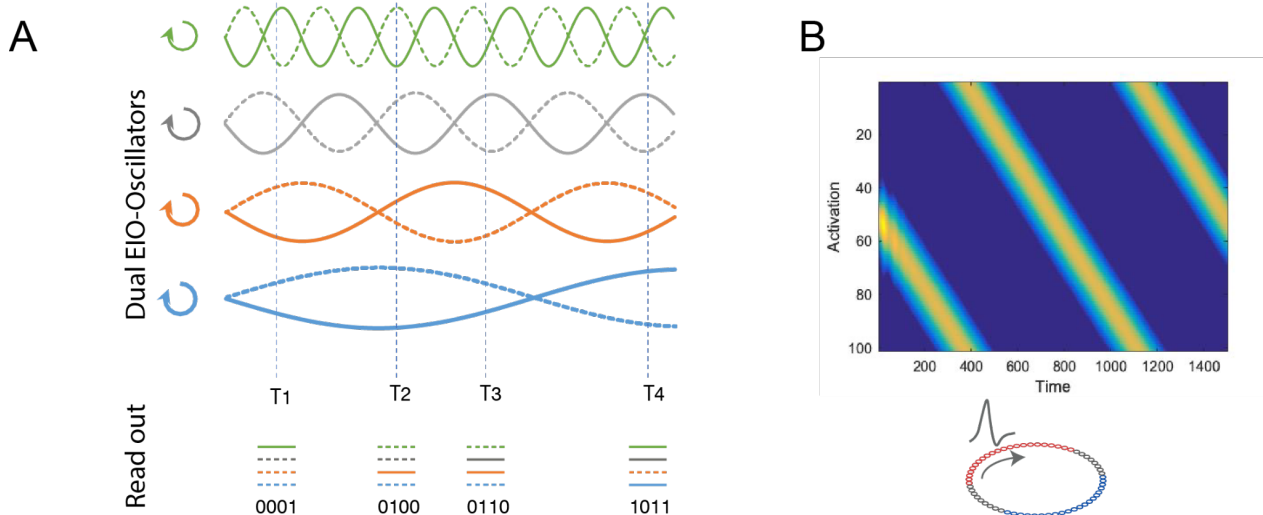
739
740   **Figure 2.** Possible neural oscillators for tracking time. (**A**) An ensemble of excitatory–inhibitory oscillation (EIO)-
741   based neurons oscillates at their endogenous frequencies. The excitatory patterns can serve as read-out of the point
742   events (adapted from Gu et al., 2015; Matell & Meck, 2004). Note, the 'OFF' phase of one oscillator is co-represented
743   by the 'ON' phase of a correspondent opponent oscillator (solid vs dashed) (**B**) A ring attractor network with strong
744   recurrent connections. The neurons are arranged in a ring and connected with distance-dependent connection weights
745   to all other neurons. The firing of a neuron inhibits all other neurons and strongly excites neurons close to it (the bottom
746   panel with red color for excitation and blue color for inhibition). With appropriate connection weights and short-term
747   synaptic plasticity, the firing activities propagate as a traveling wave (Dieterich et al., 2018; Seeholzer et al., 2017;
748   York & van Rossum, 2009; Zhang, 1996). The traveling wave exhibits similar oscillatory characteristics with temporal-
749   order information (the upper panel simulates a ring attractor with 100 neurons).
750

A Clock Stage
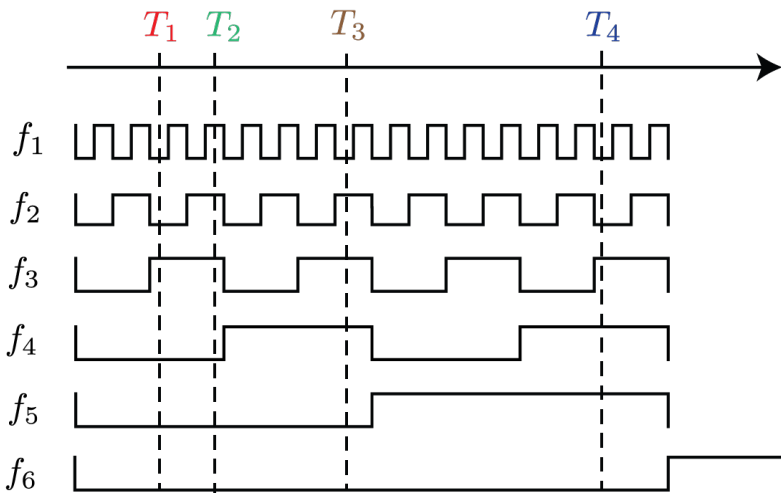
B Memory Stage
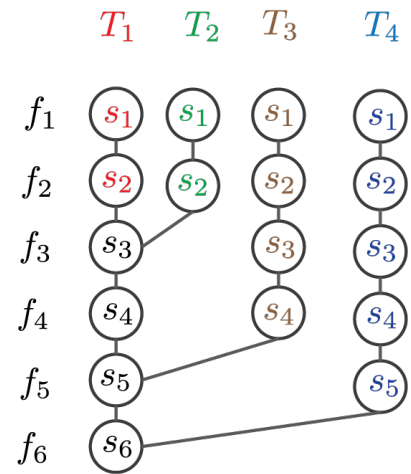
Figure 3. A schematic illustration of multifrequency oscillators for encoding time. (A) A set of log-spacing half-phase signals engendered by multifrequency excitatory–inhibitory oscillation (EIO) oscillators. A realization of the two states could be an attractor network with opponent EIOs. When a critical event occurs $(T_1, T_2, T_3\ldots)$, the read-out of the phases of the EIO oscillators are then transferred to memory with the associated event. (B) In the memory stage, those read-out nodes are stored in a shared memory for efficient representation (illustrated by colored nodes and the line connection). Nodes from the readout that do not differ from the previous nodes in the low-frequency oscillators will share the same memory representation. Such shared representation is sparse and computationally efficient. It also engenders the scalar property (see details in the text).